Hindawi
International Journal of Aerospace Engineering
Volume 2023, Article ID 9421399, 13 pages
https://doi.org/10.1155/2023/9421399

Research Article

A Modified Cycle Slip Detection Method with GNSS Doppler Assistance and Optimizing by Adaptive Threshold and Sliding Polynomial Fitting

Kezhao Li,[1] **Yunyan Shen**,[1] **Xiaokui Yue**,[2] **Yingxiang Jiao**,[1] **Kai Wang**,[1] **Zhe Yue**,[1] **and Keke Xu**[1]

[1]*School of Surveying and Land Information Engineering, Henan Polytechnic University, Jiaozuo 454000, China*
[2]*Northwestern Polytechnical University, Xi'an 710072, China*

Correspondence should be addressed to Kezhao Li; kz@hpu.edu.cn and Yunyan Shen; yunyanshen@home.hpu.edu.cn

Received 17 April 2023; Revised 29 June 2023; Accepted 12 July 2023; Published 24 July 2023

Academic Editor: Gang Wang

Cycle slip determination plays an important role in high-precision data processing and application of global navigation satellite systems (GNSS). The TurboEdit method consists of the Melbourne-Wubbena (MW) and the geometry-free phase (GF) combination. It can correctly detect and repair cycle slip in most cases. Cycle slip detection (CSD) with GF is disturbed by severe ionospheric delay variations; moreover, CSD or cycle slip repair (CSR) with the MW faces the risk of the disturbance from large pseudorange errors. Hence, cycle slip determination would be difficult under some extreme conditions, e.g., cycle slips occur in low altitude satellite, low sampling rate of dual-frequency observations. To overcome the limitations, a new dual-frequency CSD and CSR method is proposed. The main contents are as follows: (1) compared with the MW method, the Doppler-assisted phase subtraction pseudorange (DAPSP) method that we proposed has no detection blind spot and can effectively reduce the influence of pseudorange noise at high sampling rates; thus, we replace MW by the DAPSP method to improve the detection accuracy. (2) An adaptive threshold model with root mean square (RMS) is established to effectively reduce the missing and false range detection of cycle slip. (3) The sliding polynomial fitting-assisted GF (SPFAGF) is carried out according to the satellite altitude angle. The trend of ionospheric delay and residual multipath effect error between adjacent epochs is extracted and suppressed by SPFAGF. The method combined with DAPSP and SPFAGF (DAPSP-SPFAGF) overcomes the situation that the TurboEdit method cannot effectively detect under extreme conditions. The experimental results of Beidou dual-frequency observation data show that the TurboEdit method and the DAPSP-SPFAGF method can perform CSD and CSR in most cases. At the sampling rate of 1 s, the detection speed of DAPSP-SPFAGF method is significantly faster than TurboEdit method. The number of false positives about CSD is reduced from 68 to 0. At the sampling rate of 30 s and under the condition of the observed satellite altitude angle below 30°, the false alarm rate of the DAPSP-SPFAGF method is 0, but the TurboEdit method's false alarm rate is 71.2%. So DAPSP-SPFAGF method is prior to the TurboEdit method at the high sampling rates or under extreme conditions, especially it can accurately detect and repair cycle slip and reduce the false positives and false alarm rate.

1. Introduction

Compared with other global navigation satellite systems (GNSS), Beidou global navigation satellite system (BDS-3) provides more high-quality services besides positioning, navigation, and timing (PNT) services [1], such as regional information communication, global short message communication, global search and rescue service (SAR), regional precise point positioning (PPP) service, embedded satellite-based enhanced service (BDSBAS), and space environment monitoring function [2–4]. For the precise services such as positioning, navigation, orbit determination, SAR, and PPP, all need to be provided by phase observation. Thus, continuous phase observation data without cycle slip must

be required to ensure the consistency and convergence of the above precise services [5]. Therefore, CSD and CSR are still an indispensable part of GNSS data processing. However, CSD is particularly difficult in low altitude angle observation data because of high measurement noise, multipath effects, and large ionospheric delay.

The methods of CSD and CSR include the high order time difference method [6], wavelet analysis [7–9], polynomial fitting method [10–12], phase subtraction pseudorange method, Doppler integration method, TurboEdit method, and second-order, time-difference phase ionospheric residual (STPIR) method. However, different methods have different limitations. The polynomial fitting method is not suitable for small cycle slip detection [13]. The phase subtraction pseudorange method [14, 15] is affected by pseudorange noise and satellite altitude angle. Hence, it is difficult to detect small cycle slips under the strong noise environment. The Doppler integration method is affected by the low sampling rate, and the detection effect is not valid when the sampling rate is low [16, 17]. The TurboEdit method [18–21] uses Melbourne-Wubbena (MW) combination and the geometry-free (GF) phase to jointly detect cycle slips. It has high detection and repair accuracy. However, the method also has some limitations caused by their own combination of MW and GF. MW combination has insensitive cycle slip. Pseudorange noise may lead to missing and false range detection of cycle slip about low satellite altitude angle data. GF can detect small cycle slips. However, it is vulnerable to the influence of ionospheric errors. It also has multivalue characteristic and insensitivity. Therefore, TurboEdit method is not suitable for cycle slip detection with respect to the low altitude angle observation data [22]. Although the STPIR method [23–27] is simple and reduces the impact of ionospheric errors, however, its effectiveness depends on the changes of the ionosphere.

In view of the limitations of the above methods, compared with the MW method, the Doppler-assisted phase subtraction pseudorange (DAPSP) method, which can effectively reduce the influence of pseudorange noise at high sampling rates, is proposed. The selection of threshold is vital to the accuracy of cycle slip detection. The existing methods usually select empirical threshold, which has poor adaptability and is easy to cause cycle slip false detection for data under low satellite altitude angle or low sampling rate. Using sliding window filtering to make the error distribution of the test statistics more reasonable, then the size of the RMS is determined. The adaptive threshold model is built according to the RMS to reduce the missing and false range detection of the cycle slip; in order to solve the problem that DAPSP is not effective for small cycle slip detection at low sampling rate and low satellite altitude angle, a sliding polynomial fitting-assisted GF (SPFAGF) method is proposed. Although the influence of the ionospheric delay and the restriction of the satellite altitude angle about GF can be restrained by SPFAGF, the multivalue problems still exist. The DAPSP cycle slip detection model can overcome the problems of multivalue. So, we use DAPSP and SPFAGF to jointly detect and repair cycle slips (hereinafter referred to as DAPSP-SPFAGF combination method), which can detect any cycle slip effectively and is not affected by sampling rate and satellite altitude angle. Finally, the Beidou multifrequency observation data are used to verify the performance of the combination method.

2. TurboEdit Cycle Slip Detection Method

The TurboEdit method is one of the most commonly used methods for dual-frequency cycle slip processing at present. Using MW and GF combination to jointly construct the model to detect cycle slips is the principle of TurboEdit method. The TurboEdit method has high-accuracy properties of detection and repair. However, when the sampling rate is low, or the observed satellite altitude angle is low, or the ionosphere is active, the TurboEdit method will lead to false or missing detection. Thus, we will propose an improved combination method based on TurboEdit method, called DAPMP-SPFAGF, to overcome TurboEdit method's defects. Here, the key principle of TurboEdit method is introduced first.

2.1. MW Combination Method Principle. According to literature [19], the test statistics of MW combination is

$$N_{\mathrm{WL}} = \frac{L_{\mathrm{WL}}}{\lambda_{\mathrm{WL}}} = \varphi_1 - \varphi_2 - \frac{f_1 \cdot P_1 + f_2 \cdot P_2}{\lambda_{\mathrm{WL}}(f_1 + f_2)}, \tag{1}$$

where L_{WL} is the carrier phases expressed as ranges, φ_1 and φ_2 are carrier phase measurements, P_1 and P_2 indicate pseudorange measurements, f_1 and f_2 indicate the frequency of the band, λ_{WL} is the wide-lane wavelength, and N_{WL} is the ambiguity of wide-lane combination.

Recursive formula is used to calculate the average ambiguity and RMS of wide-lane combination of each epoch:

$$\begin{aligned} \bar{N}_{\mathrm{WL}}(i) &= \bar{N}_{\mathrm{WL}}(i-1) + \frac{1}{i}\left[N_{\mathrm{WL}}(i) - \bar{N}_{\mathrm{WL}}(i-1)\right], \\ \sigma^2(i) &= \sigma^2(i-1) + \frac{1}{i}\left[\left(N_{\mathrm{WL}}(i) - \bar{N}_{\mathrm{WL}}(i-1)\right)^2 - \sigma^2(i-1)\right], \end{aligned} \tag{2}$$

where $\bar{N}_{\mathrm{WL}}(i)$ is the average value of the ambiguity of wide-lane combination in the previous i epochs and $\sigma^2(i)$ represents the variance of the previous i epochs. If the two conditions in Equation (3) are met, cycle slip can be detected.

$$\left.\begin{aligned} &\left|N_{\mathrm{WL}}(i) - \bar{N}_{\mathrm{WL}}(i-1)\right| \geq 4\sigma(i-1) \\ &\left|N_{\mathrm{WL}}(i) - N_{\mathrm{WL}}(i+1)\right| \leq 1 \end{aligned}\right\}. \tag{3}$$

According to Equation (3), the ratio between the change of ambiguity of MW and the RMS can be expressed as [26]

$$D = \frac{\left|N_{\mathrm{WL}}(i) - \bar{N}_{\mathrm{WL}}(i-1)\right|}{\sigma(i-1)}. \tag{4}$$

When $D \geq k$, generally k value is ±4, means that there are cycle slips.

2.2. GF Combination Method Principle. The GF mainly uses the ionospheric residual of the dual-frequency carrier phase observation data to make a difference between adjacent epochs. Then, we can detect whether there are cycle slips. The ionospheric residual can be expressed as

$$\varphi_{\mathrm{GF}} = \varphi_1 - \frac{f_1}{f_3} \cdot \varphi_2 = N_1 - \frac{\lambda_1}{\lambda_3} N_3 + \Delta_I, \tag{5}$$

where φ_{GF} is the construction quantity of GF, f_1 and f_3 can be considered as the frequencies of B1 and B3, and Δ_I is the ionospheric residual.

The GF is calculated by the difference between adjacent epochs of Equation (5):

$$D_{\mathrm{GF}} = \varphi_{\mathrm{GF}}(t+1) - \varphi_{\mathrm{GF}}(t) = \Delta N_1 - \frac{f_1}{f_3} \Delta N_3 + \Delta_{\mathrm{ion}}, \tag{6}$$

where D_{GF} is the test statistics of GF, t represents the current epoch, $t+1$ represents the next epoch, and Δ_{ion} represents the interepoch ionospheric residual.

3. DAPSP-SPFAGF Combined Method for Detecting and Repairing Cycle Slip

The specific steps of DAPSP-SPFAGF combined method are as follows: (1) DAPSP is used for preliminary cycle slip detection about the observed data. When DAPSP test statistics exceeds the adaptive threshold, it is regarded as cycle slip and rounded up. Moreover, the observed data is preliminarily repaired by DAPSP. (2) SPFAGF is used to detect and repair the cycle slips of the observed data after DAPSP preliminary repair. When SPFAGF test statistics exceeds the threshold, it is regarded as cycle slip. And the cycle slip cannot be detected or false repaired by DAPSP, which is repaired by SPFAGF.

3.1. Model of DAPSP Method. According to literature [28], the integer ambiguity of phase subtracting pseudorange method can be expressed as

$$N_{\mathrm{PSP}} = \frac{(\lambda\varphi - P) - (I_\phi - I_P) - (\varepsilon_\phi - \varepsilon_p)}{\lambda}. \tag{7}$$

For the observation data with the same frequency, their ionospheric errors, measurement noise, and multipath effect errors are very similar between adjacent epochs. The cycle slips of subsequent epochs all contain the total cycle slips about the previous epoch. Therefore, the adjacent epoch difference calculation about Equation (7) can greatly reduce the above errors. The calculation can also eliminate the total cycle slip from the beginning epoch to the previous epoch, preserving only the tiny residuals and the cyclic slip difference between the previous epoch and the current epoch [29]. At this time, the adjacent epoch difference can be expressed as:

$$\Delta N_{\mathrm{PSP}} = N_{i+1} - N_i = \varphi_{i+1} - \varphi_i - \frac{(P_{i+1} - P_i) + \Delta\varepsilon}{\lambda}, \tag{8}$$

where ΔN_{PSP} is the test statistic of phase subtracting pseudorange method. Due to the existence of $\Delta\varepsilon$, ΔN_{PSP} is not 0. Its value should fluctuate within a small range. If cycle slip occurs in actual conditions, its value will exceed the specified range. Therefore, cyclic slip can be detected by determining whether ΔN_{PSP} is larger than the threshold value.

The phase subtracting pseudorange method is not easily affected by sampling rate, but the influence of pseudorange noise and satellite altitude angle cannot be ignored. To solve this problem, DAPSP, which is based on the combination of the Doppler integral method and phase subtraction pseudorange method to improve the detection accuracy of cycle slip, is proposed.

The integral value of Doppler is recorded as $\Delta\mathrm{dopp}_{i+1}$, and its value is obtained from Equation (8):

$$\Delta\mathrm{dopp}_{i+1} = \lambda\Delta\varphi = \lambda \cdot \int_i^{i+1} d(t)dt \approx \frac{1}{2}\lambda\Delta t(F_i + F_{i+1}), \tag{9}$$

where F is the change rate of instantaneous carrier phase measurements, $\Delta\varphi$ is the difference of carrier phase measurements between two adjacent epoch, $d(t)$ is the Doppler observation value, and t_i is the epoch of observation.

When there is no cycle slip between the i and $i+1$ epochs, the difference between $\lambda\Delta\varphi$ and $\Delta dopp_{i+1}$ only includes the observation noise, and it should fluctuate within a certain range. Then, the test statistic of the Doppler integration method is

$$\Delta N_{\mathrm{dopp}} = \Delta\varphi - \frac{\Delta\mathrm{dopp}_{i+1}}{\lambda}, \tag{10}$$

where ΔN_{dopp} is the test statistic of the Doppler integral method.

As can be seen from Equation (7), the phase subtraction pseudorange method is affected by pseudorange noise, ionospheric delay, multipath error, and other factors. When the sampling rate is high and the ionospheric change is not significant, the effects of ionospheric delay and multipath error are negligible. On this occasion, the phase subtraction pseudorange method is mainly affected by the pseudorange noise. The Doppler observation is the first derivative of the carrier phase measurements. And the Doppler integration method is proposed because of its stability and not affected by cycle slip. However, the Doppler integral method is easy to be affected by the sampling rate, because it is easy to appear false detection under low sampling rate. Thus, we combine the Doppler integration method and the phase subtraction pseudorange method to detect cycle slips.

$$\Delta N_{\mathrm{DAPSP}} = \begin{cases} \min\left[\left|\Delta N_{\mathrm{PSP}}\right|, \left|\Delta N_{\mathrm{dopp}}\right|\right] & 1\mathrm{s} \le R \le 5\mathrm{s}, \\ \Delta N_{\mathrm{PSP}} & R > 5\mathrm{s}, \end{cases} \tag{11}$$

where $\Delta N_{\mathrm{DAPSP}}$ is the test statistic of DAPSP, R is the sampling rate of data, min is the abbreviation of minimum, and min [] is the minimum value of a function.

When the sampling interval is longer than 5 s, the Doppler integration method will produce sharp fluctuations. At this time, using the Doppler integration method to assist will affect the cycle slip detection and repair; thus, the phase subtraction pseudorange method is directly used.

DAPSP is different from the traditional cycle slip detection method. Hence, we cannot use experience threshold of traditional method, and new threshold should be constructed. The DAPSP has high noise under low satellite altitude angle and low sampling rate; thus, we use the moving average filtering model to reduce the interference of high noise data about the cycle slip detection. Only the data in the window is used to calculate the average value and RMS value. And the window slides backward with the epoch.

$$\begin{aligned}\overline{\Delta N}(i) &= \frac{1}{m}\sum_{j=-m}^{-1}\Delta N(i+j),\\ \sigma^2(i) &= \frac{1}{m}\sum_{j=-m+1}^{0}\left(\Delta N(i+j)-\overline{\Delta N}(i)\right)^2,\end{aligned} \tag{12}$$

where $\overline{\Delta N}(i)$ and $\sigma^2(i)$ are the mean and mean square values about the test statistics for previous i epoch in the noncycle slip observation window, respectively, and m is the sliding window width involved in the average calculation. Through a lot of experiments, it has a good effect when the window width is 25 epochs. When $i < m$, only $\Delta\bar{N}(i)$ and $\sigma^2(i)$ of the previous i epochs are calculated.

The ratio between the rate of change about test statistics and the RMS is

$$M = \frac{\Delta N(i) - \overline{\Delta N}(i-1)}{\sigma(i-1)}. \tag{13}$$

The key of DAPSP to detect cycle slip is $|M| \geq k$; hence, the threshold expression $m_{\Delta N}$ about DAPSP is

$$m_{\Delta N} = \overline{\Delta N}(i-1) \pm k\sigma(i-1). \tag{14}$$

When the residual error caused by noise or low satellite altitude angle is large, cycle slip false detected will be caused. Thus, the noise level of the observation data needs to be considered when we set the threshold. We test the noncycle slip observation data under different satellites and different sampling rates and calculate the $|M|$ and RMS about each group of data. Figure 1 shows the statistical results under different sampling rates.

As can be seen from Figure 1 that when k is fixed, if k is set small, it is easy to cause cycle slip false detection. And if k is set larger, it is not sensitive to detection small cycle slips. Both will cause negative effects on the positioning. When the sampling rate is different, the fluctuation range of $|M|$ is different; hence, it is necessary to build different threshold models under different sampling rates. To minimize cycle slip false detection and miss detection, we build an adaptive threshold model which changes with the RMS and the sampling rate.

Determine k as shown by the black line in Figure 1. The k is as follows:

When R = 1s,

$$k = \begin{cases} 150 - 11000\sigma & 0 \leq \sigma < 0.01,\\ 70 - 3000\sigma & 0.01 \leq \sigma < 0.02,\\ 18 - 400\sigma & 0.02 \leq \sigma < 0.03,\\ 9\text{-}100\sigma & 0.03 \leq \sigma < 0.06,\\ 3 & \sigma \geq 0.06. \end{cases} \tag{15}$$

When R = 30s,

$$k = \begin{cases} 5 & 0 \leq \sigma < 0.4,\\ 6.6 - 4\sigma & 0.4 \leq \sigma < 0.9,\\ 3 & \sigma \geq 0.9, \end{cases} \tag{16}$$

where R is the size of the sampling rate.

3.2. Model of SPFAGF Method. The test statistic of GF is approximately a smooth curve if there is no cycle slip, and the sliding polynomial fitting method can effectively suppress the effects of ionospheric delay and satellite altitude angle. The ionospheric residual between adjacent epochs is large under low satellite altitude angle. Hence, when the satellite altitude angle is less than 40°, slip polynomial fitting is performed for the test statistic of GF, and the fitted value Q_{GF} is found. According to our analysis of many experimental results, it has a good suppression effect under different sampling rates when the window width is set to 30 epochs, and the polynomial coefficient is 2. The difference between the true value and the fitted value is taken as the test statistic of the SPFAGF, which is $D_{\mathrm{GF}} - Q_{\mathrm{GF}}$.

Since the ionospheric residual by SPFAGF is small, the fixed threshold can be used as the threshold of SPFAGF. According to the error propagation law, the mean square error of GF is $m_{\mathrm{GF}} = \sqrt{2m_\varphi^2 + 2(f_1^2/f_3^2)m_\varphi^2} \approx 0.0224$ cycles. Taking the mean square error of 4 times test statistic as the threshold, the threshold is 0.09 cycles.

4. Example and Analysis

This paper is verified by the BDS dual-frequency experimental data. The data acquisition time is 2021-12-27, and the acquisition location is on the roof of the national key experimental building of Henan Polytechnic University. The acquisition equipment is the CHC NAVIGATION I90 GNSS. The data acquisition interval is 1 s, and there are 6100 epochs in total. The BDS C21 satellite observation data is selected for experimental analysis because it is a MEO satellite, and MEO satellite can better reflect the impact of satellite altitude angle to cycle slip detection. Two experimental schemes are designed to verify the correctness, effectiveness, and applicability about the DAPSP-SPFAGF combined method.

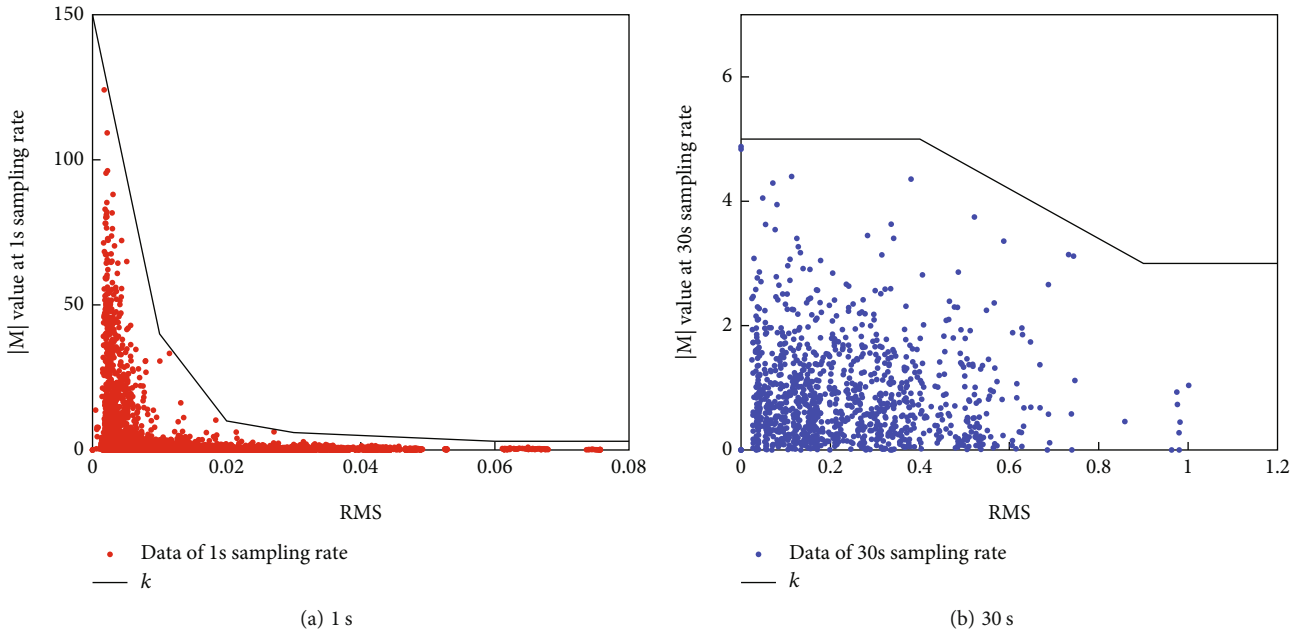

(a) 1 s (b) 30 s

Figure 1: $|M|$ value change of DAPSP using different sampling rates.

(1) Scheme 1: DAPSP-SPFAGF combination method is directly used to detect and repair cycle slips about observation data. The basic performance of DAPSP-SPFAGF combination method about cycle slip detection and repair is verified by comparing it with the TurboEdit method. When the TurboEdit method averages the full epoch of MW, the systematic deviation on BDS satellite will have a large impact to the average value and RMS, resulting false or missing detection of cycle slips [30]. Therefore, the threshold setting about TurboEdit method in scheme 1 adopts the improvement method by literature [27] to reduce the impact of cycle slip false detection. The noncycle slip phase data is obtained through the TurboEdit method and DAPSP-SPFAGF combination method. At the same time, the sampling rate of noncycle slip experiment data is reduced to 30 s, and the experimental data under the low sampling rate is obtained

(2) Scheme 2: after obtaining noncycle slip experimental data of 1 s and 30 s sampling rates, we first verify whether the DAPSP-SPFAGF combination method and the TurboEdit method will have cycle slip false detection under different sampling rates. As there are a few and single kind cycle slips in the observation data, by adding various random cycle slips to noncycle slip experimental data, the effectiveness and applicability of the DAPSP-SPFAGF combination method to detection and repair cycle slip are further verified. In order to test the actual detection effect of the DAPSP-SPFAGF combination method and TurboEdit method under low satellite altitude angle, cycle slips are artificially added to the low satellite altitude angle observation data under 1 s and 30 s sampling rates, respectively, as shown in Table 1. The cycle slips added in Table 1 are insensitive cycle slip combinations and small cycle slips of the GF combination, and if the TurboEdit method and DAPSP-SPFAGF combination method can detect the cycle slips added in Table 1, then the large cycle slips can also be effectively detected and repaired

4.1. Scheme 1 Results and Analysis. The detection results of TurboEdit method under raw data are shown in Figure 2. As shown in Figure 2(a), using the threshold of MW will pose a threat to the correctness of cycle slip detection under low satellite altitude angle. And it will result in a lot of false alarms even without real cycle slips. Besides, the MW is vulnerable to cases when the cycle slips are the same. By using the adaptive threshold of literature [27], cycle slip false detection has been reduced. However, there is still a possibility about false detection under low satellite altitude angle. In Figure 2(b), cycle slip combination is detected at the 1614th epoch by GF. The GF combination works collaboratively with the MW combination to separate cycle slips.

The detection result of DAPSP method alone using raw data is shown in Figure 3(a). As shown in Figure 3(a), DAPSP detects cycle slip combination of (2, 2) at the 1614th epoch, and DAPSP can independently repair cycle slips.

Detection result of SPFAGF method alone using raw data is shown in Figure 3(b). According to Figure 3(b), cycle slip combination is detected at the 1614th epoch by SPFAGF. However, SPFAGF, like GF, can neither distinguish the frequency on which the cycle slip occurs nor determine the size of the cycle slip. Thus, SPFAGF combination cannot independently repair cycle slips.

Table 1: Manually add cycle slip.

1 s sampling rate		30 s sampling rate	
Epoch	Add cycle slip	Epoch	Add cycle slip
6010	(5, 4)	175	(5, 4)
6020	(9, 7)	180	(9, 7)
6030	(0, 1)	185	(0, 1)
6040	(1, 0)	190	(1, 0)
6050	(1, 1)	195	(1, 1)
6060	(-1, -1)	200	(-1, -1)

As shown in Figure 4(a), DAPSP is unaffected by satellite altitude angle at 1 s sampling rate; DAPSP can detect the same cycle slips that MW cannot detect. Moreover, the DAPSP is promising to detect cycle slips at a single frequency. As shown in Figure 4(b), SPFAGF method detects that there is no cycle slip in the phase data repaired by the DAPSP method, and we can obtain the noncycle slip phase data. Compared to the TurboEdit method (shown in Figure 2), the DAPSP-SPFAGF combination method provides to reduce false alarms at low satellite altitude angle.

4.2. Scheme 2 Results and Analysis. The performance of DAPSP-SPFAGF combination method and TurboEdit method at different sampling rates is determined by using the noncycle slip phase data. First, the TurboEdit method is used for cycle slip detection about the noncycle slip phase data at different sampling rates, and the results are shown in Figure 5. As shown in Figure 5(a), the accuracy of cycle slip detection under low satellite altitude angle will be threatened by using MW, and MW will cause various cycle slip false detections. As shown in Figure 5(d), we can see a great number of detected cycle slips by GF. We think the detected cycle slips are false alarms due to the rapid variation of the ionosphere because we use the noncycle slip experiment data, and no jump for MW is seen. In a nutshell, the TurboEdit method will increase number of false alarms in cycle slip detection under disturbed ionospheric conditions. The false alarms will then impact the reinitializing the ambiguity. Although the method of reinitializing the ambiguity is simple and convenient, the convergence time required to achieve high accuracy depends on the method of processing the observed data. In poor cases, it can reach tens of minutes to reach the converged accuracy. Thus, the TurboEdit method will lead to poor availability of high-precision positioning result under disturbed ionospheric conditions.

The detection results of DAPSP-SPFAGF combination method about the noncycle slip phase data using different sampling rates are shown in Figure 6. As can be seen from Figures 6(a) and 6(c), if a fixed threshold is used, a large fixed threshold should be set in order to avoid misjudgment; then, it will not be possible to effectively detect small cycle slips of data with high sampling rate. However, using adaptive threshold can effectively detect cycle slips of data at different sampling rates and altitude angles according to RMS, and it can effectively reduce cycle slip missed detection and false detection.

Compared with MW combination (shown in Figures 5(a) and 5(c)), the cycle slip false detection under low satellite altitude angle will be reduced by DAPSP (shown in Figures 6(a) and 6(c)). Comparing Figure 5(d) with Figure 6(d), we can see that using the GF to detect cycle slips is significantly affected by the disturbed ionospheric conditions, but SPFAGF suppresses this effect well. Although the fixed threshold is 0.09 cycles, SPFAGF has a good detection effect under disturbed ionospheric conditions. Thus, the DAPSP-SPFAGF combination method significantly reduces the false detection of cycle slips compared with the TurboEdit method. At the sampling rate of 1 s, the detection time of TurboEdit method is 90922 μs, the DAPSP-SPFAGF combination takes 56375 μs, and the time delay of TurboEdit method and PRP-STMGF method processing each epoch is 14.91 μs and 9.24 μs, respectively. Thus, the DAPSP-SPFAGF method has a shorter time delay than the TurboEdit method when detecting and repairing periodic slip on per epoch. At the sampling rate of 1 s, the number of false alarms is reduced from 68 to 0. At the sampling rate of 30 s and under the condition of the observed satellite altitude angle below 30°, the false alarm rate of the DAPSP-SPFAGF method is 0, but the TurboEdit method's false alarm rate is 71.2%.

Both the DAPSP-SPFAGF combination method and TurboEdit method can effectively detect the manually added cycle slips under high satellite altitude angle. Due to the limited space, more description is not needed. Next, we verify the detection effect of the two detection methods on manually added cycle slips under low satellite altitude angle.

Detection results of TurboEdit method after adding cycle slip combination using different sampling rate are shown in Figure 7. Figures 7(a) and 7(d) show that the TurboEdit method results a lot of cycle slip false detections at low satellite altitude angles, regardless of the 1 s or 30 s sampling rate. Thus, cycle slips of low satellite altitude angle are not effectively detected and repaired by the TurboEdit method, and the data quality is affected.

Figure 8 exhibits the detection results of DAPSP-SPFAGF combination method after adding cycle slip combination using different sampling rates. As shown in Figure 8(a), DAPSP still keeps good detection effect at low satellite altitude angle. And the DAPSP can effectively detect and repair cycle slips of any cycle, detecting large cycle slips at epochs 6010 and 6020, small cycle slips at epochs 6030 and 6040, and cycle slips of the same size at epochs 6050 and 6060. Compared with the MW (shown in Figure 7(a)), cycle slip false detections are reduced by DAPSP (shown in Figure 8(a)), and the DAPSP has no detection blind spot. Besides, DAPSP could detect and repair cycle slips of any cycle independently and accurately at 1 s sampling rate, and it is not affected by satellite altitude angle. As shown in Figure 8(b), the test statistics of SPFAGF after repairing phase data with DAPSP is totally within the limit.

At 30 s sampling rate, DAPSP cannot effectively detect small cycle slips because of sampling interval, but the cycle slips over 4 cycles can still be effectively detected using it (shown in Figure 8(c)). As shown in Figure 8(d), SPFAGF still has a good detection effect to small cycle slips at 30 s sampling rate. However, SPFAGF has multivalued problems,

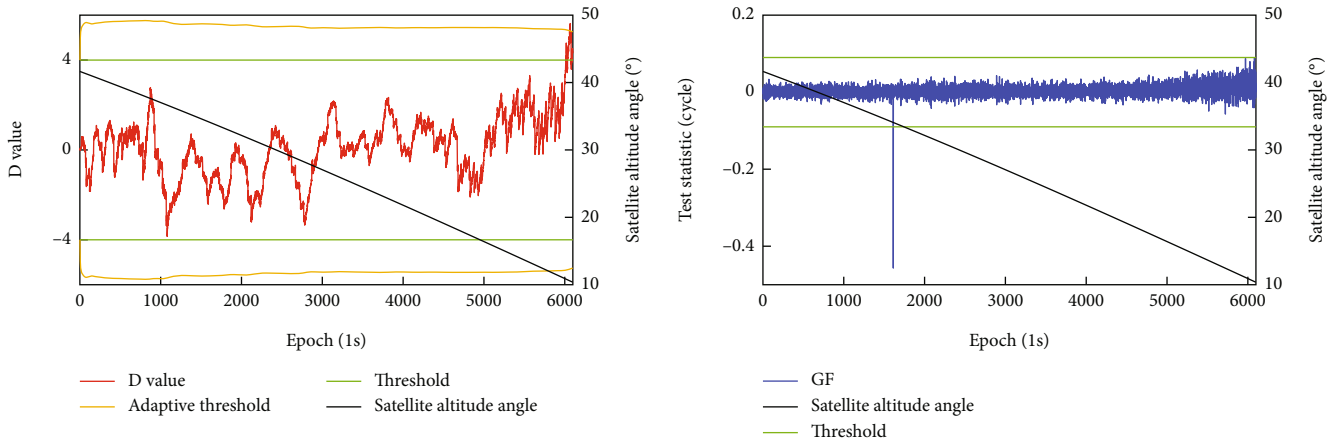

(a) Detection result by MW combination

(b) Detection result by GF combination based on the result by MW combination

Figure 2: Detection results of TurboEdit method using raw data.

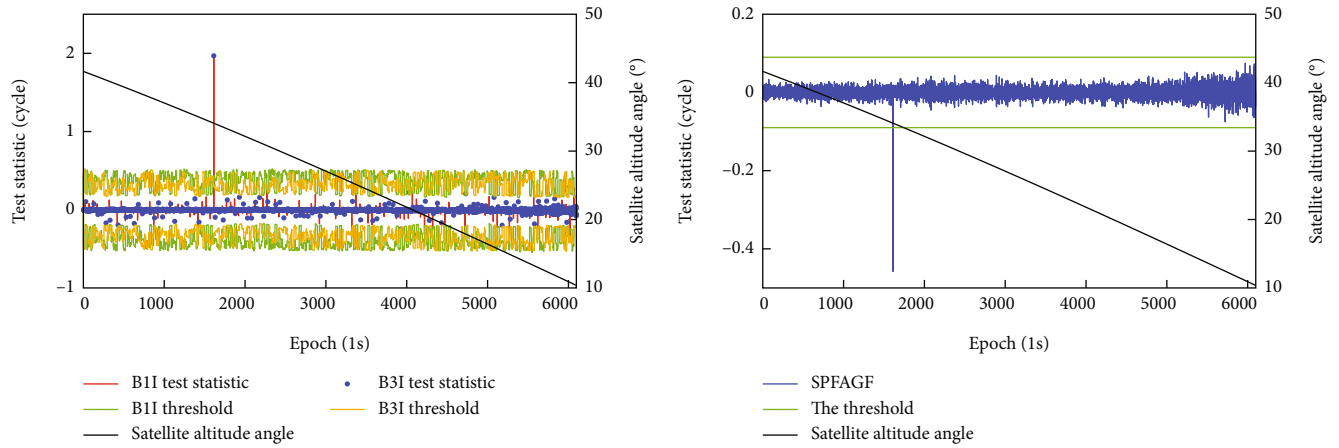

(a) Detection result by DAPSP method

(b) Detection result by SPFAGF method

Figure 3: Detection results of DAPSP and SPFAGF alone using raw data.

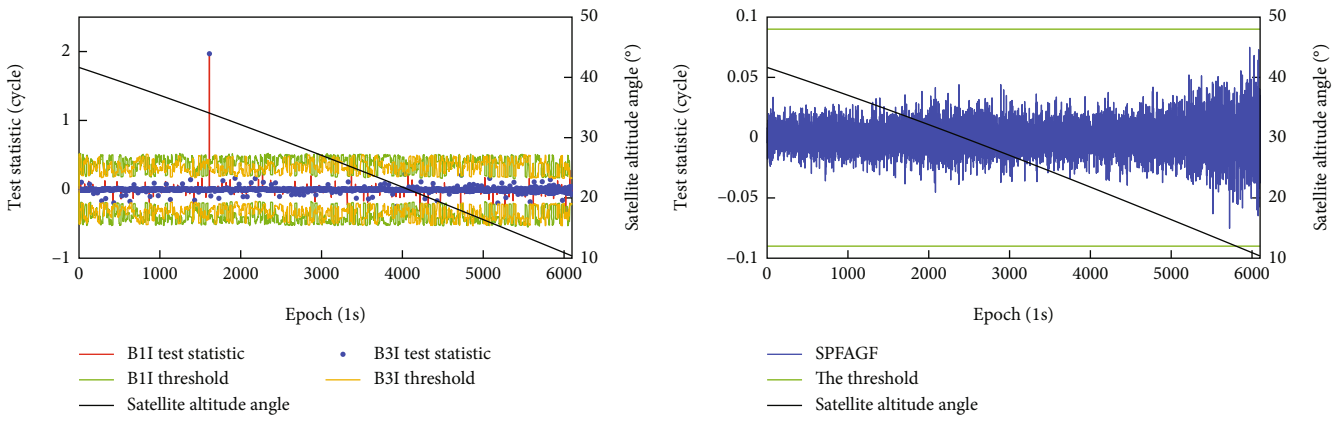

(a) Detection result by DAPSP method

(b) Detection result by SPFAGF method based on the result by DAPSP method

Figure 4: Detection results of DAPSP-SPFAGF combination method using raw data.

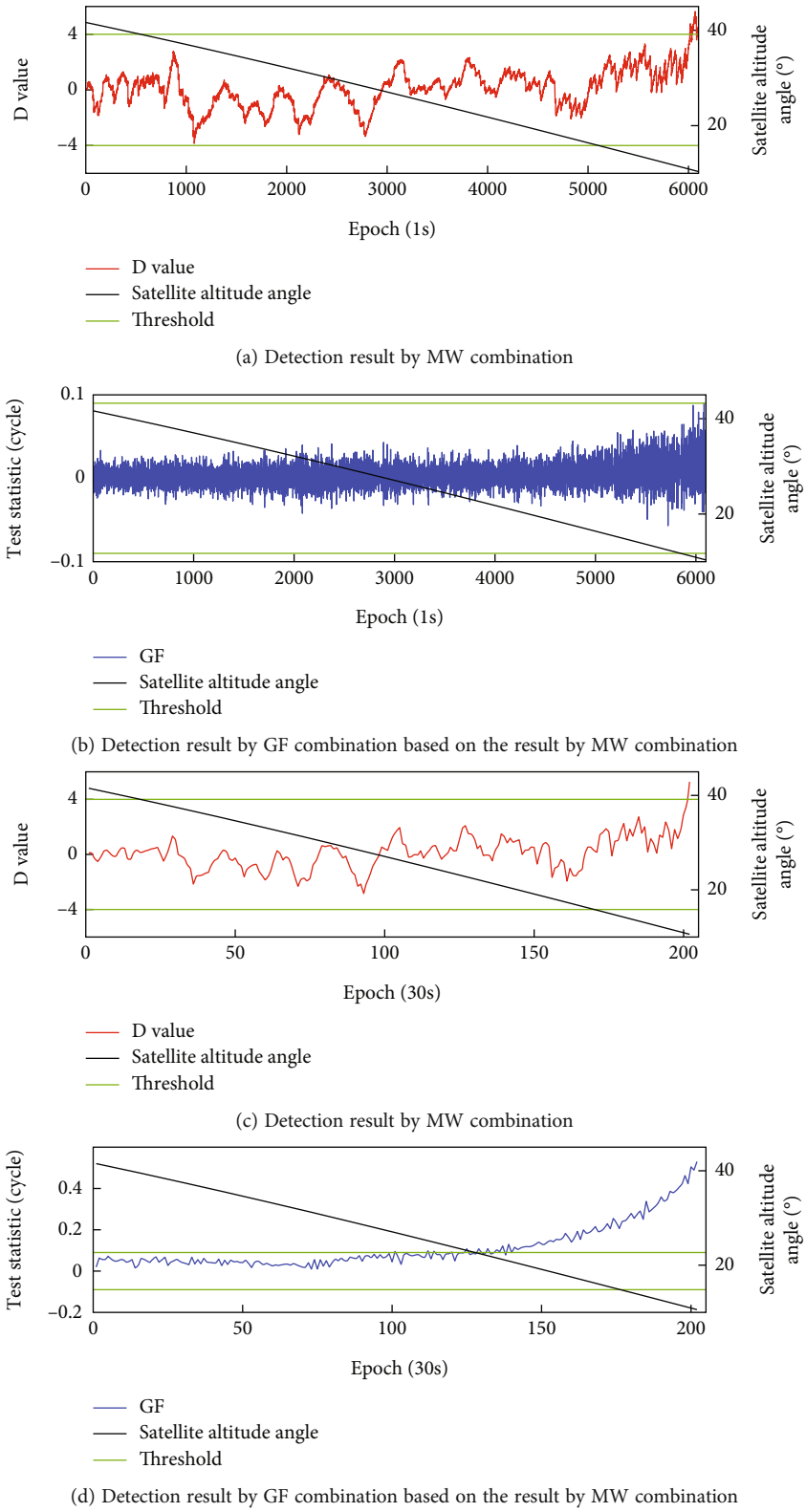

(a) Detection result by MW combination

(b) Detection result by GF combination based on the result by MW combination

(c) Detection result by MW combination

(d) Detection result by GF combination based on the result by MW combination

Figure 5: Detection results of TurboEdit method about the noncycle slip experiment data using different sampling rates.

which lead to it can only exactly determine the cycle slips within four cycles. Thus, the SPFAGF works collaboratively with the DAPSP to complement each other to accurately detect and repair all artificially simulated cycle slip combinations.

The results of DAPSP-SPFAGF combined method to detect and repair cycle slips at 30 s sampling rate are shown in Table 2, and the test statistic about undetected cycle slip is taken as 0. Table 2 shows the false detections and missing

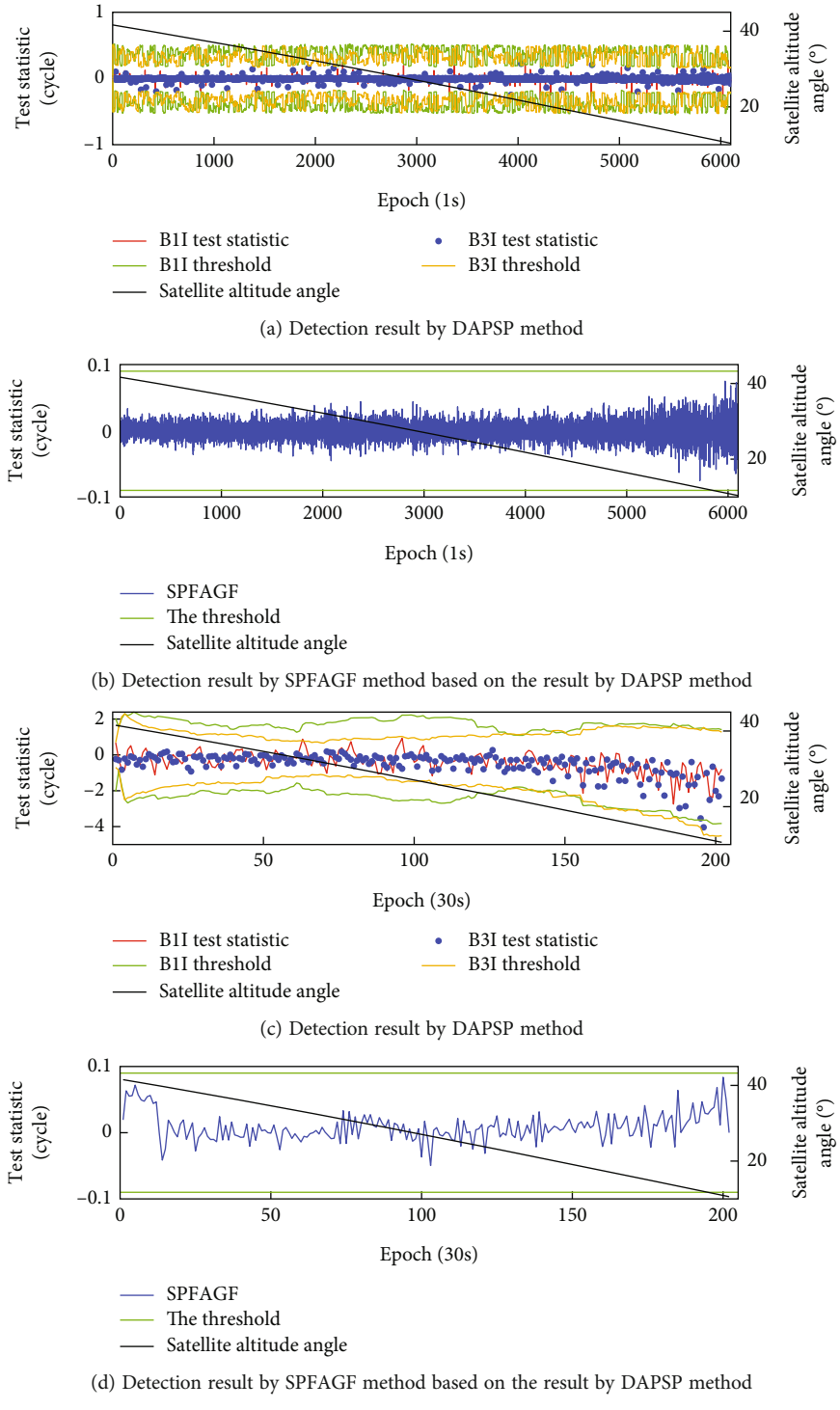

(a) Detection result by DAPSP method

(b) Detection result by SPFAGF method based on the result by DAPSP method

(c) Detection result by DAPSP method

(d) Detection result by SPFAGF method based on the result by DAPSP method

Figure 6: Detection results of DAPSP-SPFAGF combination method about the noncycle slip experiment data using different sampling rates.

detections about DAPSP which will be detected and repaired by SPFAGF, and the DAPSP-SPFAGF combined method can effectively detect various cycle slips even under low satellite altitude angle and low sampling rate.

At 1 second sampling rate, the DAPSP is not influenced by the factor of the satellite altitude angle and can detect any kinds of cycle slips. With the decrease of sampling rate and the increase of pseudorange noise, the detection accuracy of DAPSP decreases. And the small cycle slips cannot be detected by it, but the cycle slips over 4 cycles can still be effectively detected using it. GF can detect small cycle slips at a low sampling rate, but the false or miss detection phenomena will occur under the conditions of strong ionosphere or low satellite altitude angle. SPFAGF combination

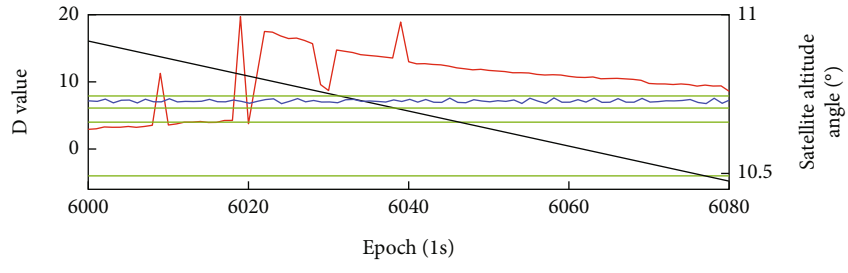

(a) Detection result by MW combination

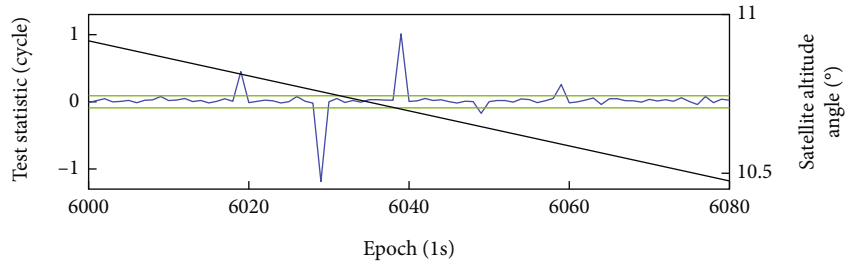

(b) Detection result by GF combination based on the result by MW combination

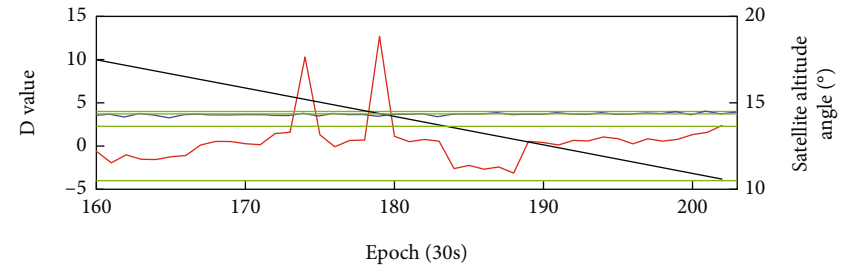

(c) Detection result by MW combination

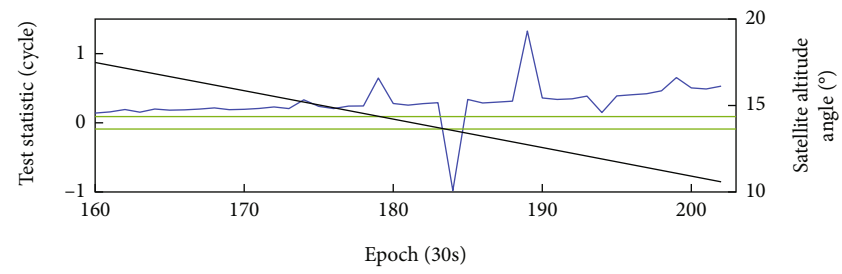

(d) Detection result by GF combination based on the result by MW combination

Figure 7: Detection results of TurboEdit method after adding cycle slip combination using different sampling rates.

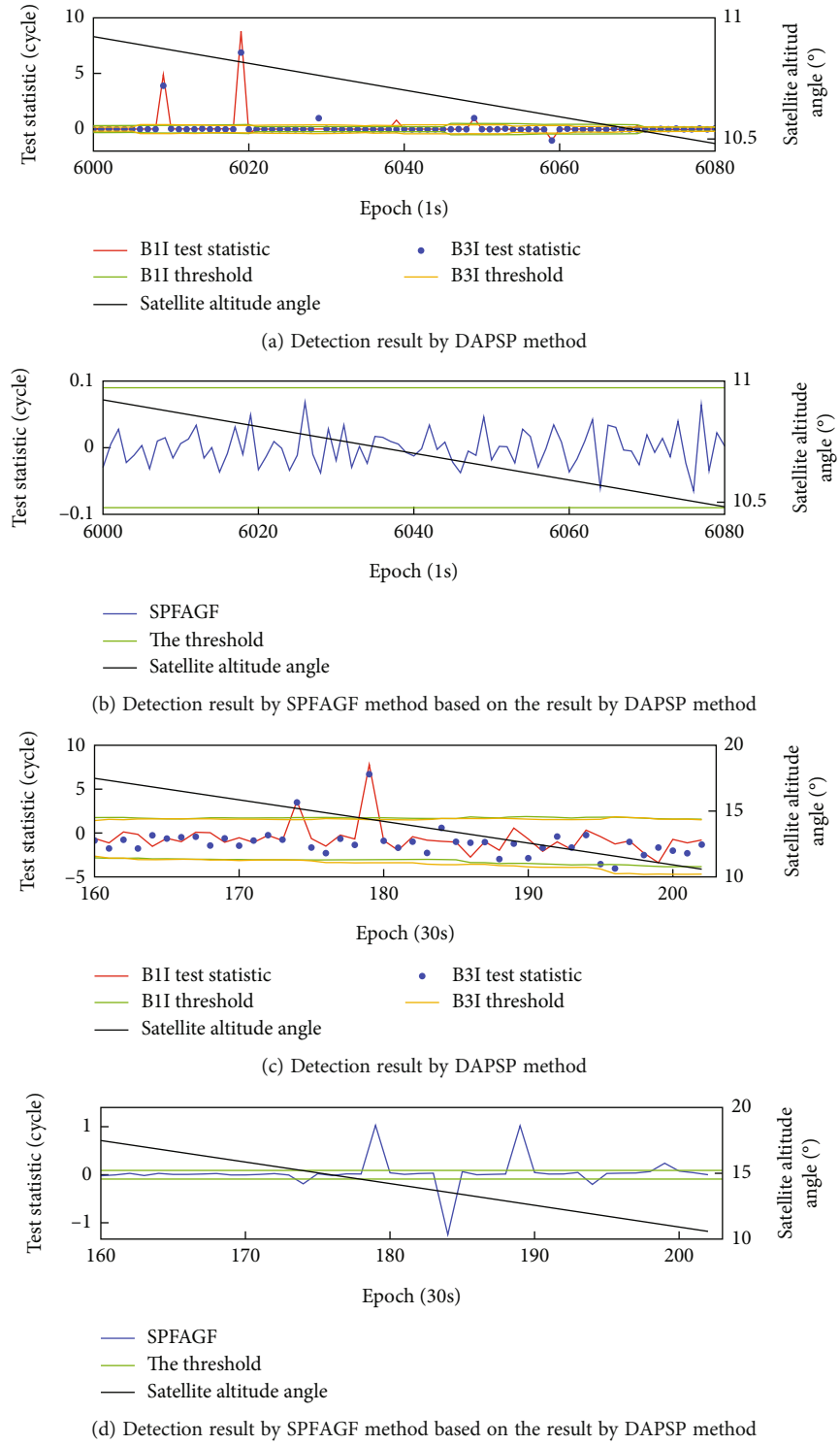

Figure 8: Detection results of DAPSP-SPFAMGF combination method after adding cycle slip combination using different sampling rates.

can effectively suppress the influence of ionospheric delay, especially the influence of the observation satellite altitude angle about GF. However, GF and SPFAGF both have multivalued problems, which lead to the combinations can only exactly determine the cycle slips within four cycles [31]. As mentioned above, DAPSP can still detect cycle slips more than 4 cycles even under extreme conditions; hence, combining with DAPSP, the multivalue problem of SPFAGF can be solved. The combination of the DAPSP and SPFAGF improves the performance and accuracy of cycle slip detection and repair.

Table 2: Cycle slip repair statistics of DAPSP-SPFAGF combined method at 30 s sampling rate.

Epoch	Add cycle slip	Test statistic of DAPSP	Cycle slip value of DAPSP	Test statistic of SPFAGF	Cycle slip value of SPFAGF
175	(5, 4)	(3.64, 3.49)	(4, 3)	-0.19	(1, 1)
180	(9, 7)	(7.80, 6.71)	(8, 7)	1.03	(1, 0)
185	(0, 1)	(0, 0)	(0, 0)	-1.25	(0, 1)
190	(1, 0)	(0, 0)	(0, 0)	1.02	(1, 0)
195	(1, 1)	(0, 0)	(0, 0)	-0.20	(1, 1)
200	(-1, -1)	(0, 0)	(0, 0)	0.23	(-1, -1)

5. Conclusions and Outlook

Cycle slips inevitably occur because of the temporary failure of lock in the GNSS receiver carrier tracking loop, low signal-to-noise ratio, and active ionosphere. Whatever the reason for the cycle slips, cycle slips should be detected and repaired before the carrier phase observation is used in the GNSS high-precision positioning application. If we directly apply the TurboEdit method widely used to detect and repair cycle slip, there will emerge many failures caused by severe ionospheric delay and low satellite altitude angle. To solve above problem, a new cycle slip detection and repair method (DAPSP-SPFAGF combined method) is proposed to overcome the disturbances by severe ionospheric delay and low satellite altitude angle. The method consists about DAPSP and SPFAGF.

(1) DAPSP model is proposed, and an adaptive threshold model that changes with RMS is constructed. DAPSP is not affected by satellite altitude angle and has high accuracy under 1 s sampling rate. DAPSP can independently detect and repair cycle slips of any cycle at 1 s sample rate, which improves the cycle slip detection accuracy. According to constructing an adaptive threshold model that changes with RMS, the cycle slip false detection and miss detection can be effectively reduced under low satellite altitude angle or low sample rate

(2) SPFAGF model is proposed to suppress the influence about severe ionospheric delay and low satellite altitude angle on GF. The low satellite altitude angle observation data has some shortcomings, such as large measurement noise and multipath effect and severe ionospheric delay; there will be many false detection and missing detection of cycle slips by GF. To solve above problem, we first select the appropriate window width and polynomial coefficients; then, we perform sliding polynomial fitting to the test statistic of GF. We finally take the difference between the true value and the fitted value as the test statistic of SPFAGF. Through practical verification, the SPFAGF can effectively suppress the influence of severe ionospheric delay and low satellite altitude angle on GF

Many compared experiments are carried out with the dual-frequency data, and the DAPSP-SPFAGF combined method's ability to resist the disturbances of severe ionospheric variation and low satellite altitude angle is verified. Compared with TurboEdit method, DAPSP-SPFAGF combined method can detect and repair cycle slips in low satellite altitude angle and low sampling rate and reduce the false and missed alarms of cycle slip.

Data Availability

The datasets analyzed in this study are managed by the School of Surveying and Land Information Engineering, Henan Polytechnic University, and can be available on request from the corresponding authors.

Conflicts of Interest

The authors declare that they have no conflict of interest.

Authors' Contributions

KL designed the proposed algorithm and drafted the very first manuscript. YS significantly implemented part of the algorithm and provided the software platform. ZY collected all experimental raw measurements. The experimental network is being established and maintained by YJ and KW. XY and KX revised the manuscript. All authors read and approved the final manuscript.

Acknowledgments

The authors would like to thank C. K, who is a professor at The Ohio State University, for providing the valuable advice. This research was funded by the National Natural Science Foundation of China (Grant Nos. 41774039 and 42204040), the State Key Lab Project of China (no. 6142210200104), and the Key Project of Science and Technology of Henan (no. 212102210085). The support is gratefully acknowledged.

References

[1] Y. Yang, Y. Mao, and B. Sun, "Basic performance and future developments of BeiDou global navigation satellite system," *Satellite Navigation*, vol. 1, no. 1, p. 1, 2020.

[2] Y. X. Yang, W. Gao, S. Guo, Y. Mao, and Y. Yang, "Introduction to BeiDou-3 navigation satellite system," *Navigation*, vol. 66, no. 1, pp. 7–18, 2019.

[3] Y. X. Yang, Y. Yang, X. Hu, C. Tang, L. Zhao, and J. Xu, "Comparison and analysis of two orbit determination methods for

BDS-3 satellites," *Acta Geodaetica et Cartographica Sinica*, vol. 48, no. 7, pp. 831–839, 2019.

[4] Y. Yang, Y. Yang, X. Hu et al., "Inter-satellite link enhanced orbit determination for BeiDou-3," *Journal of Navigation*, vol. 73, no. 1, pp. 115–130, 2020.

[5] D. Li, Y. Dang, Y. Yuan, and J. Mi, "A new cycle-slip repair method for dual-frequency BDS against the disturbances of severe ionospheric variations and pseudoranges with large errors," *Remote Sensing*, vol. 13, no. 5, p. 1037, 2021.

[6] A. Kleusberg, Y. Georgiadou, F. van den Heuvel, and P. Heroux, *GPS Data Preprocessing with DIPOP 3.0. Internal Technical Memorandum*, Department of Surveying Engineering, University of New Brunswick, Fredericton, New Brunswick, Canada, 1993.

[7] H. Dingfa and Z. Jiancheng, "Wavelet analysis for cycle slip detection and reconstruction of GPS carrier phase measurements," *Acta Geodaetica et Cartographica Sinica*, vol. 26, no. 4, pp. 73–78, 1997.

[8] C. Changsheng and G. Jingxiang, "Cycle-slip detection and correction of GPS data by wavelet transform," *Geomatics and Information Science of Wuhan University*, vol. 32, no. 1, pp. 39–42, 2007.

[9] H. Bingjie, L. Lintao, and G. Guangxing, "Detection of cycle-slip in the GPS precise point positioning based on wavelet transform," *Geomatics and Information Science of Wuhan University*, vol. 31, no. 6, pp. 512–515, 2006.

[10] H. Lichtenegger and B. Hofmann-Wellenhof, "GPS-data preprocessing for cycle-slip detection," in *Global Positioning System: An Overview. International Association of Geodesy Symposia*, Y. Bock and N. Leppard, Eds., vol. 102, Springer, New York, NY, 1990.

[11] M. Li, X. W. Gao, and G. Xu Ai, "An improved method of the polynomial fitting of the cycle slip," *Science of Surveying and Mapping*, vol. 33, no. 4, pp. 82-83, 2008.

[12] P. Jing, M. Ying, and L. Chun, "Research and improvement of polynomial fitting method in cycle slip detection," *Journal of Electronic Measurement and Instrument*, vol. 31, no. 11, pp. 1828–1834, 2017.

[13] F. Wei, L. Hua, D. Xinggan, and H. Dingfa, "An improved method of detecting and repairing carrier phase cycle slip," *Science of Surveying and Mapping*, vol. 35, no. 6, pp. 39–41, 2010.

[14] S. Han, "Quality-control issues relating to instantaneous ambiguity resolution for real-time GPS kinematic positioning," *Journal of Geodesy*, vol. 71, no. 6, pp. 351–361, 1997.

[15] G. Shuliang, H. Zhigang, and L. Rui, "Cycleslips detecting approach for single frequency GPS users," *Journal of Beijing University of Aeronautics and Astronautics*, vol. 37, no. 8, pp. 1021–1025, 2011.

[16] Z. Dai, "MATLAB software for GPS cycle-slip processing," *GPS Solutions*, vol. 16, no. 2, pp. 267–272, 2012.

[17] S. Chunming and W. Aisheng, "Detect cycle slips using Doppler integration," *Urban Geotechnical Investigation and Surveying*, vol. 1, pp. 24–26, 2006.

[18] Z. Liu, "A new automated cycle slip detection and repair method for a single dual-frequency GPS receiver," *Journal of Geodesy*, vol. 85, no. 3, pp. 171–183, 2011.

[19] G. Blewitt, "An automatic editing algorithm for GPS data," *Geophysical Research Letters*, vol. 17, no. 3, pp. 199–202, 1990.

[20] I. Lei, L. Zulong, M. Changsong, J. Chenchen, J. Ke, and P. Xiong, "An improved algorithm for real-time cycle slip detection and repair based on TurboEdit epoch difference model," *Geomatics and Information Science of Wuhan University*, vol. 46, no. 6, pp. 920–927, 2021.

[21] X. Xu, Z. Nie, Z. Wang, and Y. Zhang, "A modified TurboEdit cycle-slip detection and correction method for dual-frequency smartphone GNSS observation," *Sensors*, vol. 20, no. 20, p. 5756, 2020.

[22] Z. Zhang, J. Zeng, B. Li, and X. He, "Principles, methods and applications of cycle slip detection and repair under complex observation conditions," *Journal of Geodesy*, vol. 97, no. 5, 2023.

[23] C. Cai, Z. Liu, P. Xia, and W. Dai, "Cycle slip detection and repair for undifferenced GPS observations under high ionospheric activity," *GPS Solutions*, vol. 17, no. 2, pp. 247–260, 2013.

[24] Z. Fan, L. Changjian, F. Xu, Xu, and Yangyin, "Cycle slip detection and repair based on front-to-back sliding window filtering and second-order time-difference phase ionospheric residua method," *Science of Surveying and Ma*, vol. 44, no. 7, pp. 53–58, 2019.

[25] C. Chenglin, S. Wenbo, Z. Wuling, Y. Honggang, and X. X. Ping, "Detect and repair cycle-slip by reconstruction Doppler integral algorithm and STPIR," *Acta Geodaetica et Cartographica Sinica*, vol. 50, no. 2, pp. 160–168, 2021.

[26] F. Lihong, W. Li, Z. Ming, and Z. Zengji, "A combination of MW and second-order time-difference phase ionospheric residual for cycle slip detection and repair," *Geomatics and Information Science of Wuhan University*, vol. 40, no. 6, pp. 790–794, 2015.

[27] Z. Xiaohong, Z. Qi, H. Jun, and K. Chao, "Improving TurboEdit real-time cycle slip detection by the construction of threshold model," *Geomatics and Information Science of Wuhan University*, vol. 42, no. 3, pp. 285–292, 2017.

[28] K. Yang, Z. Lü, L. Li, Y. Kuang, and W. Xu, "Doppler integration aided kinematic single-frequency cycle slip detection," *Geomatics and Information Science of Wuhan University*, vol. 47, no. 11, pp. 1860–1869, 2021.

[29] W. Sifan, L. Jianzhang, and S. Zhemin, "Research on detection and reparation for cycle slip in BDS observations using combination of phase ionospheric residual method and phase reduce pseudorange method," *Journal of Navigation and Positioning*, vol. 9, no. 5, pp. 89–95, 2021.

[30] Z. Chenxi, D. Yamin, X. Shuqiang, and Z. Longping, "An improved BDS cycle slip detection method based on TurboEdit," *Science of Surveying and Mapping*, no. 6, pp. 47–52, 2021.

[31] Y. Dong, P. Dai, S. Wang et al., "A study on the detecting cycle slips and a repair algorithm for B1/B3," *Electronics*, vol. 10, no. 23, p. 2925, 2021.